J. Plasma Physics (2009), *vol.* 75, *part* 1, *pp.* 71–84.
doi:10.1017/S0022377808007502 Printed in the United Kingdom

Dynamic behaviour of an oxygen dc discharge

A. RICHTER[1], H. TESTRICH[1], H.-E. WAGNER[1], D. LOFFHAGEN[2] and C. WILKE[2]

[1] Institute for Physics, University of Greifswald, Felix-Hausdorff-Straße 6, 17489 Greifswald, Germany
[2] INP Greifswald, Felix-Hausdorff-Straße 2, 17489 Greifswald, Germany
(richter@physik.uni-greifswald.de)

(Received 19 November 2007 and in revised form 6 May 2008, first published online 12 August 2008)

Abstract. The dynamic behaviour of a positive column oxygen plasma is investigated both experimentally and theoretically. In the experiment the response of the discharge current to small external perturbations of the electrical field is measured. Using these data the electrical impedance of the plasma is obtained dependent on the frequency of the external perturbation. A drift approximation model is presented, which covers the experimental findings over a wide range of the perturbation frequency. It appears that the influence of the fluctuations of the neutral species is negligible and the dynamic behaviour of the plasma is mostly governed by the charged particles. This provides a simple expression for the plasma impedance which allows the reaction rate and transport coefficients, as well as discharge parameters, to be validated.

1. Introduction

Oxygen plays a prominent role in electronegative plasmas. There are various technical applications for oxygen and plenty of data (such as electronic cross sections) is available. This paper is devoted to the study of a positive column plasma of an oxygen dc discharge.

Most investigations of oxygen plasmas focus on the equilibrium properties of the plasma [1–6], such as the spatial structure or chemical composition. Considerably fewer studies are concerned with the plasma stability [7–9]. Owing to the numerous reaction channels involved, oxygen plasmas require quite complex models and thus gaining a simple insight into the physics of the plasma is difficult. Since in every self-consistent model the particle densities are coupled by the corresponding reaction rates it is usually difficult to evaluate the influence of a certain process.

The analysis of the dynamic plasma behaviour provides a possibility to cut off most of the plasma chemistry and to concentrate on the dominant charged particles only [10, 11]. In this way one gains the possibility to validate single reaction rates and to examine their influence on the plasma behaviour. This approach has been applied to an oxygen dc discharge with discharge parameters in the range $0.75\,\text{Torr cm} < pr_0 < 1.75\,\text{Torr cm}$ for the reduced pressure and $8\,\text{mA cm}^{-1} < I/r_0 < 20\,\text{mA cm}^{-1}$ for the reduced discharge current. In the experiment two probes have been placed in the positive column of the discharge to measure the axial electrical field in this plasma. To obtain a linear response of the positive column a small sinusoidal voltage, in the frequency range from 0.1 to 100 kHz, has been superimposed on the discharge voltage. The variation of the electrical field

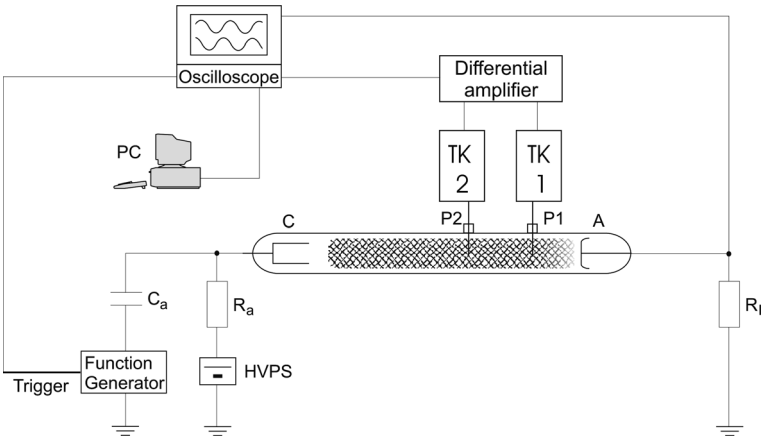

Figure 1. Experimental setup.

in magnitude and its relative phase to the discharge current were measured. From these data the reactance and resistivity, or more precisely the impedance per length unit, is readily obtained.

Impedance investigations have been applied successfully to rare gases and they helped, e.g., to clarify the interplay between stepwise and direct ionization processes [12]. In the present paper, this method is applied to electronegative plasmas for the first time. For the investigations the positive column of a cylindrical dc discharge at low currents was used because of its simplicity. However, with suitable changes this approach could be applied to more general situations as well.

Special attention has to be paid to the evaluation of the rates of the processes involving electrons. As is usually the case in low-temperature plasmas, the electrons are far from equilibrium. Therefore, the electron velocity distribution function (EVDF) and the resulting rate and transport coefficients were determined for each set of discharge parameters by solving the steady-state, spatially homogeneous electron Boltzmann equation.

After describing the experimental setup and discharge conditions in Sec. 2 a model for the dynamic behaviour of the plasma is presented in Sec. 3. Some approximations and the resulting equations are also introduced. The theoretical results are compared with the experimental findings and some implications are finally discussed in Sec. 4.

2. Experimental setup

The measurements were realized in the positive column of a pure dc oxygen discharge. Figure 1 shows the experimental setup.

The discharge was maintained in a glass tube with inner radius $r_0 = 2.5$ cm in the pressure range from 0.3 to 0.7 Torr and a discharge current between 1 and 50 mA. The distance between the electrodes was 60 cm.

An optimal cleaning of the discharge tube is necessary for reliable results. Therefore, the tube is pumped to the end pressure of about 10^{-8} Torr and subsequently heated for 24 hours at 350°C. In order to keep the experimental conditions temporally constant, the discharge was previously worked by a current of 100 mA for about an hour.

https://doi.org/10.1017/S0022377808007502 Published online by Cambridge University Press

The electrical field was measured by means of two Langmuir probes (tungsten) placed at a mutual distance of 5 cm in the positive column of the discharge. For the determination of the plasma impedance the discharge voltage was modulated with a sinusoidal signal from the function generator and the voltage drop between the two probes was measured as a function of the current. In all measurements the modulation degree was lower than 3%. The voltage drop, which is proportional to the electrical field in the positive column, was recorded by a difference amplifier. Its input consists of two active probes (TK) with a high input resistance (>5 MΩ) and low input capacitance (<1.5 pF). Simultaneously, the amplitude of the current modulation $\hat{I}$ was measured by means of the resistor R_I. In combination with the discharge resistance and the load resistor R_a the resistor R_I represents a voltage divider with a capacitance regarding the ground. The voltage divider has to be compensated for by a capacity parallel to R_I. The resistance $R_s = \hat{E}\cos\phi/\hat{I}$ and the reactance $R_c = \hat{E}\sin\phi/\hat{I}$ are determined by means of the measured voltage drop and current modulation as well as the phase shift ϕ between these two signals.

3. Model of the impedance behaviour

The discharge is characterized by the following plasma parameters. The total electron collision cross section for molecular oxygen is less than 8×10^{-16} cm^2 for all electron energies [13]. Thus, the mean free path of the electrons is smaller than 0.1 cm for the pressure range considered. This value is much smaller than the tube radius r_0 and the distance between the two probes, so that the electrons can be treated in a drift-diffusion approximation. Typical mean electron energies are somewhat lower than 4 eV. The ionization degree of the plasma is smaller than 10^{-7} and the recombination of charged particles can be neglected. The Debye length is less than about 0.05 cm and the plasma is assumed to be quasi-neutral. Energy relaxation of the electrons with respect to field variations is guaranteed up to frequencies of about 3×10^4 Hz (see [13, 14]). Therefore, the rate coefficients and collision frequencies, respectively, for electron collision processes can be chosen as a function of the reduced electric field E/N. The rate and transport coefficients of the electrons are determined by solving the spatially homogeneous, steady-state Boltzmann equation of the electrons for a given E/N and cross section data [13] using a modified version of the multiterm solution technique [15] adapted to account for non-conservative electron collision processes [16].

For the discharge conditions the main charged particles are electrons (e), positive ions (O_2^+), and negative ions (O^-). Other ions such as O^+ and O_2^- have comparatively lower concentrations (see [3, 10]). A strong link to the neutral species exists for the negative ions mainly via their detachment in collisions with oxygen atoms (O) and metastable singlet molecules ($O_2^* = O_2(a\,^1\Delta_g)$) (see [5, 17]). Therefore, the latter species have also been included in the model. Stepwise ionization, dissociation and dissociative attachment of metastable molecules compete with the direct electron collision processes of ground state molecules of O_2 only for high fractions $[O_2^*]/[O_2]$. Table 1 gives the main species included in the model, the dominant collision processes as well as the rate coefficients and wall recombination probabilities.

For the theoretical description of the dynamic behaviour of the plasma a model was derived consisting of the time-dependent balance equations for the relevant species coupled with an expression for the discharge current. Assuming axial homogeneity of the discharge plasma the discharge current is given in a drift

https://doi.org/10.1017/S0022377808007502 Published online by Cambridge University Press

Table 1. Reactions, rate coefficients and recombination probabilities at the wall used in the model calculations.

Reaction	Rate coefficient	Reference
$O_2 + e \rightarrow O_2^* + e$	$K_m(E/N)$	[13]
$O_2 + e \rightarrow O + O + e$	$K_{diss}(E/N)$	[13]
$O_2 + e \rightarrow O_2^+ + e + e$	$K_{iz}(E/N)$	[13]
$O_2 + e \rightarrow O + O^-$	$K_{att}(E/N)$	[13]
$O_2^* + e \rightarrow O_2 + e$	$K_s(E/N)$	[13] and detailed balancing
$O^- + O_2^* \rightarrow O_3 + e$	$K_{det}^m = 1.9 \times 10^{-10}\,cm^3\,s^{-1}$	[10]
$O^- + O \rightarrow O_2 + e$	$K_{det}^O = 2.3 \times 10^{-10}\,cm^3\,s^{-1}$	[10]
Reaction	**Wall recombination probability**	**Reference**
$O_2^* + \text{wall} \rightarrow O_2$	$\gamma_m = 4 \times 10^{-4}$	Estimated
$O + \text{wall} \rightarrow \frac{1}{2}O_2$	$\gamma_O = 4 \times 10^{-3}$	Estimated

approximation by the relation

$$I(t) = e_0 2\pi \int_0^{r_0} r[\mu_e N_e(r,t) + \mu_n N_n(r,t) + \mu_p N_p(r,t)]E(t)\,dr. \tag{3.1}$$

Here μ_j and $N_j(r,t)$ with $j = e, n, p$ denote the mobility and particle density, respectively, of electrons (e), negative (n) and positive (p) ions. The axial electric field strength $E(t)$ is radially constant according to Maxwell's equations. The electron mobility $\mu_e(E/N)$ was determined from the solution of the electron Boltzmann equation mentioned above. Values for the mobilities of O^- and O_2^+ in oxygen can be found in [18, 19]. Neglecting radial changes of the total gas density N and assuming quasi-neutrality, expression (3.1) reads

$$I(t) = e_0 \pi r_0^2 [(\mu_e + \mu_p)\bar{N}_e(t) + (\mu_n + \mu_p)\bar{N}_n(t)]E(t), \tag{3.2}$$

where

$$\bar{N}_j(t) = \frac{2}{r_0^2} \int_0^{r_0} r N_j(r,t)\,dr \tag{3.3}$$

is the density of species j averaged over the cross section of the discharge tube.

The corresponding balance equations describing the behaviour of the spatially averaged particle density of the prevailing species are

$$\frac{\partial \bar{N}_e(t)}{\partial t} + \frac{\bar{N}_e(t)}{\tau_e(t)} = [K_{iz}(E/N) - K_{att}(E/N)]N_{O_2}\bar{N}_e(t) + \left(K_{det}^m \bar{N}_m(t) + K_{det}^O \bar{N}_O(t)\right)\bar{N}_n(t), \tag{3.4a}$$

$$\frac{\partial \bar{N}_n(t)}{\partial t} + \frac{\bar{N}_n(t)}{\tau_n(t)} = K_{att}(E/N)N_{O_2}\bar{N}_e(t) - \left(K_{det}^m \bar{N}_m(t) + K_{det}^O \bar{N}_O(t)\right)\bar{N}_n(t), \tag{3.4b}$$

$$\frac{\partial \bar{N}_m(t)}{\partial t} + \frac{\bar{N}_m(t)}{\tau_m(t)} = K_m(E/N)N_{O_2}\bar{N}_e(t) - K_{det}^m \bar{N}_m(t)\bar{N}_n(t) - K_s(E/N)\bar{N}_m(t)\bar{N}_e(t), \tag{3.4c}$$

$$\frac{\partial \bar{N}_O(t)}{\partial t} + \frac{\bar{N}_O(t)}{\tau_O(t)} = 2K_{diss}(E/N)N_{O_2}\bar{N}_e(t) - K_{det}^O \bar{N}_O(t)\bar{N}_n(t). \tag{3.4d}$$

https://doi.org/10.1017/S0022377808007502 Published online by Cambridge University Press

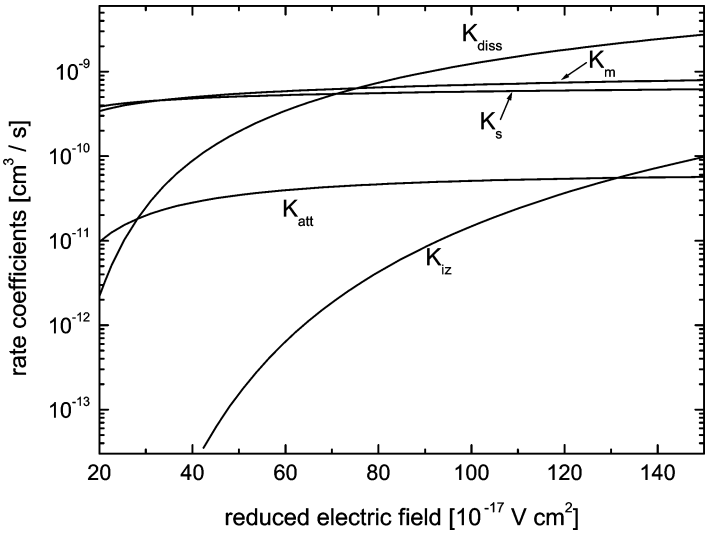

Figure 2. Rate coefficients as a function of E/N for the electron collision processes in Table 1.

In this system of coupled ordinary differential equations for electrons (e), negative ions (n), metastable molecules (m) and oxygen atoms (O), N_{O_2} is the density of ground state oxygen molecules and τ_j with $j = \mathrm{e}, \mathrm{n}, \mathrm{m}, \mathrm{O}$ denotes the lifetime due to wall loss of the respective species. This lifetime replaces the divergence of the radial flux after averaging over the cross section of the tube and is discussed below. Note that in deriving system (3.4) the spatial average of a product of two densities is approximated by the product of the average densities, because the radial profile of the neutral species is flat [17].

A balance of the positive ions is not required, because the plasma is supposed to be quasi-neutral. The argument E/N of the rate coefficients indicates that these quantities were determined by solving the electron Boltzmann equation. The dependence of the various rate coefficients on the reduced electric field is displayed in Fig. 2.

The right-hand side of system (3.4) describes the volume processes of particle gain and loss. The left-hand side takes into account the wall losses of the particles due to radial fluxes. For the electrons the radial flux to the wall j_{er} at steady state is given in the drift-diffusion approximation by the relation [20]

$$j_{\mathrm{er}}(r) = -\mu_{\mathrm{p}} \frac{D_{\mathrm{e}}}{\mu_{\mathrm{e}}} \left[1 + \alpha(r) \left(1 + \frac{\mu_{\mathrm{n}}}{\mu_{\mathrm{p}}} \right) \right] \frac{\partial N_{\mathrm{e}}(r)}{\partial r}, \tag{3.5}$$

where D_{e} is the diffusion coefficient of the electrons and $\alpha(r) = N_{\mathrm{n}}(r)/N_{\mathrm{e}}(r)$ denotes the electronegativity. The radial averaging of the divergence of $j_{\mathrm{er}}(r)$ over the cross section of the tube yields the expression

$$\frac{1}{\tau_{\mathrm{e}}} = \frac{2}{r_0} \frac{j_{\mathrm{er}}(r_0)}{\bar{N}_{\mathrm{e}}} \tag{3.6}$$

for the lifetime of the electrons. The determination of τ_{e} from this relation requires knowledge of the radial profile of the electron density, which is a challenging problem for electronegative plasmas [21]. However, the direct calculation of τ_{e} can

https://doi.org/10.1017/S0022377808007502 Published online by Cambridge University Press

be circumvented. Assuming that the radial electric field traps the negative ions, they do not reach the wall, i.e. $1/\tau_n = 0$ (see [11, 21]). Thus, the loss of negative ions by detachment has to compensate for the gain due to electron attachment in the equilibrium positive column according to (3.4b). At the same time the relation $\tau_e^{-1} = K_{iz}(E/N)N_{O_2}$ follows from (3.4a), which was employed in the present study.

The lifetime τ_j of the oxygen atoms ($j = O$) and the metastable molecules ($j = m$) can be estimated by [22]

$$\tau_j^{-1} = \frac{\gamma_j \bar{v}_j}{2r_0}, \tag{3.7}$$

where γ_j denotes the probability of recombination of the species j at the wall and $\bar{v}_j$ is its mean thermal velocity, i.e. $\bar{v}_j = (8k_B T_j/\pi M_j)^{1/2}$ with the Boltzmann constant k_B and the temperature T_j of the species of mass M_j. The values for the recombination probabilities γ_O and γ_m used in the present studies are given in Table 1. In the literature a variation by about an order of magnitude is found for these recombination probabilities on glass (see, e.g., [10, 22–24]). One reason could be their sensitive dependence on the discharge parameters and surface properties. As the wall recombination constitutes an important loss channel for the oxygen atoms and metastable oxygen molecules, the equilibrium density values of O_2^* and O as calculated by (3.4c) and (3.4d) have to be considered with special care.

Before turning to the dynamic plasma behaviour the equilibrium state is considered. The particle densities at plasma equilibrium are determined by the current balance (3.2) and the stationary balance equations (3.4b)–(3.4d) for given discharge current, pressure, tube radius and measured electric field. In the following the equilibrium values of the discharge current, electric field and particle densities are indicated by the additional index '0'. Note that for the determination of the reduced field E_0/N at equilibrium, gas heating in the active plasma also has to be taken into account. Therefore, the mean gas temperature T_g is estimated by [25]

$$T_g = 330\ \mathrm{K} + 230\ \mathrm{K}\frac{E_0 I_0}{[\mathrm{W\ cm^{-1}}]} \tag{3.8}$$

and the gas density N is obtained from the pressure p_0 by the ideal gas law.

From the expression (3.2) for the discharge current a relation for the electrical impedance per length unit Z can be derived. If the discharge is weakly externally driven, the properties of the discharge vary slightly around their equilibrium values. Thus, the temporal variation of the discharge properties can be approximated by $\bar{A}(t) = \bar{A}_0 + \tilde{A}(t)$, where $\tilde{A}(t)$ is a small correction with $\tilde{A}(t) \ll \bar{A}_0$ and A represents the discharge current, electric field and particle densities N_j with $j = e, n, m, O$. Assuming that the small field variation only has a small influence on the mobilities of the charged particles, the electrical impedance per length unit $Z = \tilde{E}(t)/\tilde{I}(t)$ of the positive column is determined from (3.2) and reads

$$Z = \frac{E_0}{I_0}\left(1 + \frac{E_0[(\mu_e + \mu_p)(\tilde{N}_e(t)/\tilde{E}(t)) + (\mu_n + \mu_p)(\tilde{N}_n(t)/\tilde{E}(t))]}{(\mu_e + \mu_p)\bar{N}_{e0} + (\mu_n + \mu_p)\bar{N}_{n0}}\right)^{-1} \tag{3.9a}$$

$$\approx \frac{E_0}{I_0}\left(1 + \frac{E_0}{\bar{N}_{e0}}\frac{\tilde{N}_e(t)}{\tilde{E}(t)}\right)^{-1}. \tag{3.9b}$$

In the approximation formula (3.9b) the estimations $\mu_e \gg \alpha\mu_j$ with $j = n, p$ were used. Apart from the equilibrium values E_0, I_0, N_{e0} and N_{n0} expression (3.9a)

https://doi.org/10.1017/S0022377808007502 Published online by Cambridge University Press

contains the ratios $\tilde{N}_e(t)/\tilde{E}(t)$ and $\tilde{N}_n(t)/\tilde{E}(t)$. These ratios have to be specified by using the time-dependent balance equations (3.4). Since the plasma equilibrium is disturbed only weakly, this set of balance equations is linearized about equilibrium with respect to the modulations of the discharge parameters. The change of the rate coefficients is also accounted for up to first order according to, e.g., $K_{iz}(E/N) = K_{iz}(E_0/N)+\tilde{E}(t)\partial K_{iz}(E/N)/\partial E|_{E_0}$. The lifetimes due to wall loss are taken at their equilibrium value because, e.g., τ_e^{-1} defined in (3.6) is directly proportional to the characteristic electron energy $u_e = e_0 D_e/\mu_e$ which in turn satisfies $E_0 \partial u_e/\partial E \ll u_e$.

All modulations are characterized by the phase frequency ω, the amplitude $\hat{N}_j$ and relative phase ϕ_j of the plasma component j with $j = e, n, m, O$ and they can be expressed by the relation $\tilde{N}_j(t) = \hat{N}_j \exp(i(\omega t+\phi_j))$. Thus, a linear, inhomogeneous system of four equations for the ratios $\tilde{N}_j(t)/\tilde{E}(t)$ results. From these ratios the phase shifts with respect to the electric field

$$\phi_j = \arctan\left(\frac{\mathrm{Im}(\tilde{N}_j(t)/\tilde{E}(t))}{\mathrm{Re}(\tilde{N}_j(t)/\tilde{E}(t))}\right) + k\pi \tag{3.10}$$

and the amplitudes of the modulations

$$\frac{\hat{N}_j/\bar{N}_{j0}}{\hat{E}/E_0} = \left|\frac{\tilde{N}_j(t)}{\tilde{E}(t)}\right| \frac{E_0}{\bar{N}_{j0}} \tag{3.11}$$

are obtained, where the phase of the electric field was set to ϕ_E=0 in (3.10). The parameter k has to be chosen to be $k = 0$ for $\mathrm{Re}(\tilde{N}_j(t)/\tilde{E}(t)) > 0$, $k = +1$ for $\mathrm{Re}(\tilde{N}_j(t)/\tilde{E}(t)) < 0$ and $\mathrm{Im}(\tilde{N}_j(t)/\tilde{E}(t)) > 0$ and $k = -1$ for $\mathrm{Re}(\tilde{N}_j(t)/\tilde{E}(t)) < 0$ and $\mathrm{Im}(\tilde{N}_j(t)/\tilde{E}(t)) < 0$. The amplitudes of the modulations in (3.11) are related to their equilibrium values and the modulation degree of the electric field.

To determine the electrical impedance Z and the related quantities given by (3.10) and (3.11), the linearized balance equations (3.4) were solved with respect to the ratios $\tilde{N}_j(t)/\tilde{E}(t)$ at given discharge current I_0, pressure p_0, tube radius r_0 and measured electric field E_0.

4. Results and discussion

Depending on the discharge conditions the positive column of an oxygen discharge exists in two modes [26]. For higher values of the discharge current the positive column of the discharge is maintained by higher electric fields (a so-called H-mode with E about $10\,\mathrm{V\,cm^{-1}}$). Decreasing the current, the positive column becomes unstable accompanied by a sudden jump to lower mean values of the electric field (the T-mode with E about $4\,\mathrm{V\,cm^{-1}}$). This transition shows a pronounced hysteresis behaviour as illustrated in Fig. 3. Here the discharge current was tuned from lower to higher values and *vice versa*. The impedance investigations discussed in the following were carried out in the H-mode regime.

Figure 4 compares the theoretical results with the experimental data for the impedance at two different discharge conditions, i.e. at (a) $p_0 = 0.7\,\mathrm{Torr}$ and $I_0 = 32\,\mathrm{mA}$ and (b) $p_0 = 0.5\,\mathrm{Torr}$ and $I_0 = 16\,\mathrm{mA}$. The resistance $R_s = \mathrm{Re}(Z)$ and reactance $R_c = \mathrm{Im}(Z)$ of the positive column are represented in a parametric plot. The impedance curves are parameterized by the frequency of the external perturbation. Each point on the curves corresponds to a frequency in the range from 0.3 to 80 kHz. The dotted line for the experimental results at discharge condition (b) indicates

https://doi.org/10.1017/S0022377808007502 Published online by Cambridge University Press

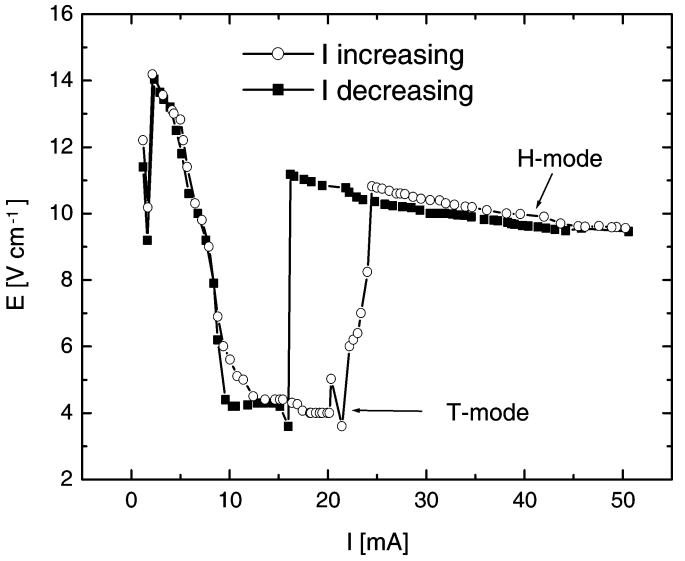

Figure 3. Measured axial electric field versus discharge current in the positive column at $p = 0.5$ Torr.

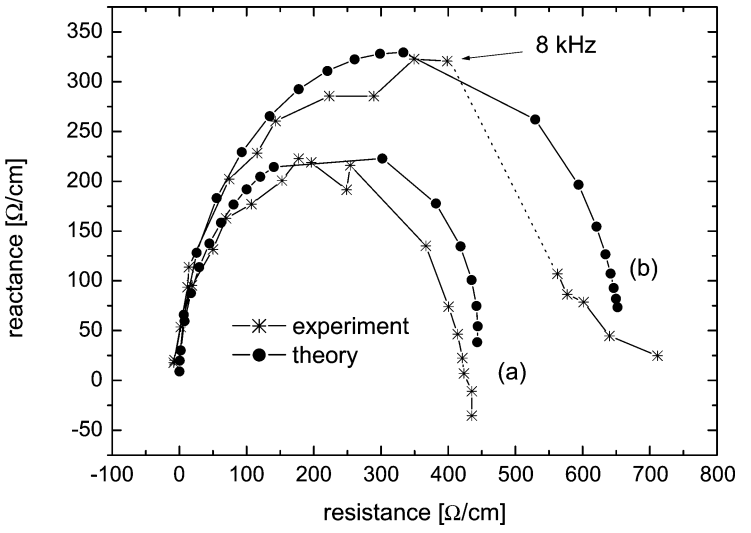

Figure 4. Impedance of the positive column parameterized by the frequency at (a) $p_0 = 0.7$ Torr and $I_0 = 32$ mA and (b) $p_0 = 0.5$ Torr and $I_0 = 16$ mA. Frequency labels from left to right: 300 Hz, $1, 2, \ldots, 9$ kHz and $10, 20, \ldots, 80$ kHz.

that in the frequency range between 8 and 40 kHz the positive column became unstable and no reliable measurements were possible for this frequency range. As can be seen from Fig. 4 the model calculations show satisfactory agreement with the experimental data over a wide range of frequencies. This confirms the theoretical approach and validates the rate coefficients used.

https://doi.org/10.1017/S0022377808007502 Published online by Cambridge University Press

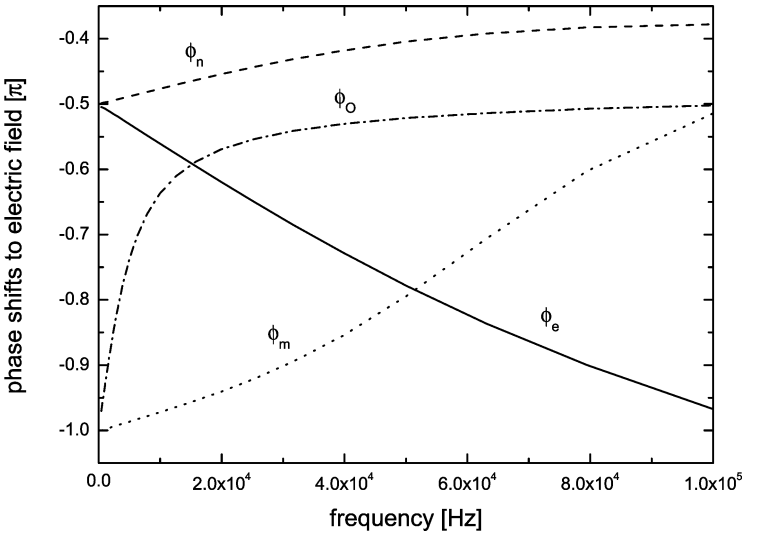

Figure 5. Calculated phase shifts to the electric field ϕ_j with $j = \mathrm{e, n, m, O}$ for electrons (e), O^- ions (n), metastable O_2^* molecules (m) and atomic oxygen (O) at $p_0 = 0.7$ Torr and $I_0 = 32$ mA.

In the following, results at the standard discharge condition, i.e. condition (a) with $p_0 = 0.7$ Torr and $I_0 = 32$ mA, are discussed in more detail. The gas temperature T_g at this condition was estimated to be about 420 K by means of (3.8) with an equilibrium electric field $E_0 = 12\,\mathrm{V\,cm^{-1}}$. Under this condition the electron mobility was calculated to be $\mu_e = 1.13 \times 10^6\ \mathrm{cm^2\ V^{-1}\ s^{-1}}$. The solution of the balance equations (3.4) for the dc discharge condition yields an equilibrium concentration of metastable oxygen molecules of 7.9% and of atomic oxygen of 2.3% of the neutral gas, respectively. For the electronegativity of the plasma, the value $\alpha = 2.2$ is found.

Applying a sinusoidal perturbation the particle densities respond in a sinusoidal manner as well, but are shifted in phase with regard to the variation of the external electric field. Figure 5 shows the phase shifts of the particle densities to the electric field ϕ_j with $j = \mathrm{e, n, m, O}$ as determined from (3.10). For frequencies up to at least 3×10^4 Hz the modulation of the mean electron energy is in phase with the modulation of the electric field. At a fixed frequency the species described by the lower lying curve precede the corresponding densities above by the difference between the curves. The phase shift between the densities of electrons and negative ions increases from zero for low frequencies to about $\pi/2$ for higher frequencies. At low frequencies the neutral species are ahead of the modulations of the electrons by $\pi/2$ and in antiphase to the mean electron energy. For higher frequencies the phase relation between electrons and neutral species is reversed and the neutral species lag in phase by $\pi/2$.

If the external perturbation is sufficiently small, the amplitudes of all modulations are expected to depend linearly on the size of the perturbation. This means that all amplitudes are mutually proportional to each other. Therefore, it is necessary to relate the amplitudes to one of the quantities. In (3.11) the amplitude of the external electric field fluctuation $\hat{E}$ was chosen for that purpose. Furthermore,

https://doi.org/10.1017/S0022377808007502 Published online by Cambridge University Press

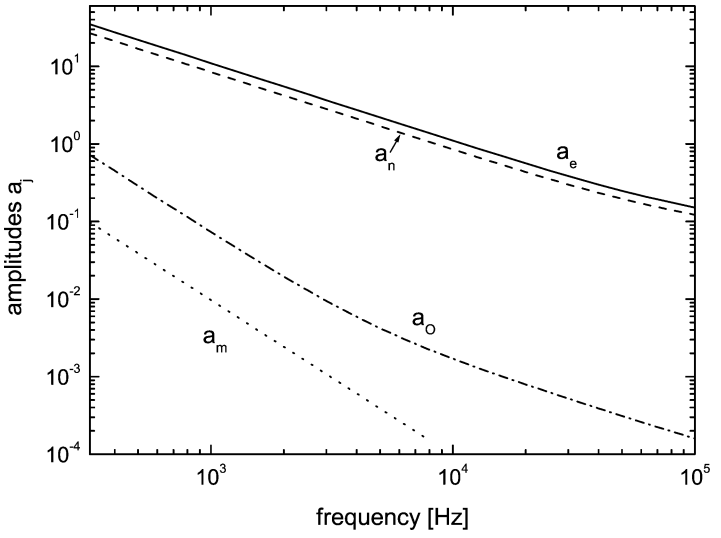

Figure 6. Frequency dependence of the calculated amplitudes $a_j = (\hat{N}_j/N_{j0})/(\hat{E}/E_0)$ with $j = \mathrm{e, n, m, O}$ for electrons (e), O^- ions (n), metastable O_2^* molecules (m) and atomic oxygen (O) under standard discharge conditions.

rather the modulation degree $\hat{N}_j/\bar{N}_{j0}$ of the particle density of species j is of physical significance than the absolute value of its amplitude $\hat{N}_j$. This is the reason for defining the dimensionless quantities (relative amplitudes) as given by (3.11).

Figure 6 shows the relative amplitudes of the fluctuations of the particle densities in dependence on the perturbation frequency. The relative amplitudes can be interpreted as the modulation degree $\hat{N}_j/\bar{N}_{j0}$ of the particle density of species j as a percentage for a given modulation degree of 1% in the electric field. The modulation degrees of the densities considered decrease with increasing frequency of the external perturbation. For frequencies f larger than 300 Hz, the modulation degree of the neutral species is at least two orders of magnitude lower than that of the charged particles. This is readily understood if one bears in mind that the main loss channel for metastable oxygen molecules O_2^* and atomic oxygen O is diffusion to the wall. From (3.7) the wall loss frequencies ($\nu_j = \tau_j^{-1}$) of the neutral species are $\nu_\mathrm{m} = 5$ Hz for the metastable molecules and $\nu_\mathrm{O} = 37$ Hz for atomic oxygen at the discharge condition considered. Comparing these wall loss frequencies to the external frequency, one can conclude that the neutral species cannot follow the rapid frequency changes. This motivates us to treat the metastable molecules and atomic oxygen as a stationary background for the dynamic behaviour of the discharge at frequencies above 300 Hz.

In the frame of this approximation of quasi-stationary detachment partners O_2^* and O their densities are described by the steady-state version of (3.4c) and (3.4d), respectively, i.e. setting $\partial\bar{N}_\mathrm{m}(t)/\partial t = \partial\bar{N}_\mathrm{O}(t)/\partial t = 0$. Then, the detachment frequency ν_det given by

$$\nu_\mathrm{det} = K_\mathrm{det}^\mathrm{m}\bar{N}_\mathrm{m} + K_\mathrm{det}^\mathrm{O}\bar{N}_\mathrm{O} \tag{4.1}$$

on the right-hand side of (3.4a) and (3.4b) becomes time-independent and the temporal variation of the charged particles is coupled to the density of metastable molecules and atomic oxygen via this frequency only. By means of this simplification and

https://doi.org/10.1017/S0022377808007502 Published online by Cambridge University Press

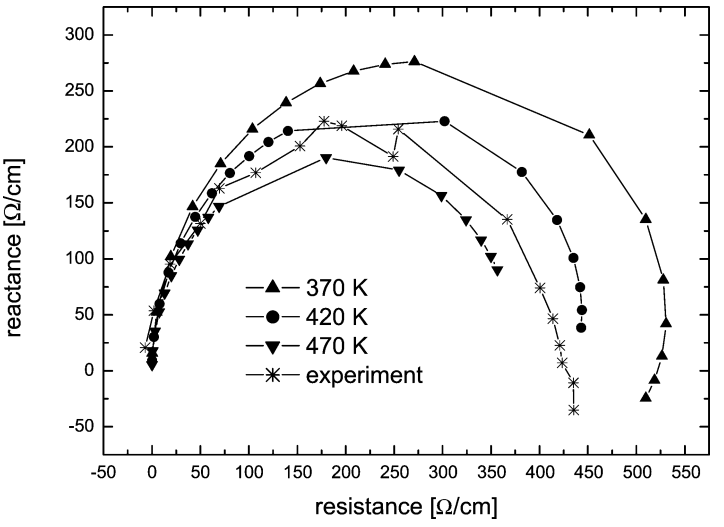

Figure 7. Influence of the gas temperature T_g on the plasma impedance parameterized by the frequency under standard discharge conditions. Frequency labels from left to right: 300 Hz, $1, 2, \ldots, 9$ kHz and $10, 20, \ldots, 80$ kHz.

starting from the approximation formula (3.9b), the plasma impedance is explicitly given by

$$Z = \frac{E_0}{I_0}\left(1 + E_0 \frac{\nu'_{\mathrm{iz}}(E_0/N)(1 - i\nu_{\mathrm{det}}/\omega) - \nu'_{\mathrm{att}}(E_0/N)}{i\omega + \nu_{\mathrm{att}}(E_0/N) + \nu_{\mathrm{det}}}\right)^{-1}, \tag{4.2}$$

where $\nu'_j(E_0/N) = \partial\nu_j(E/N)/\partial E|_{E_0}$ and $\nu_j(E/N) = N_{\mathrm{O}_2} K_j(E/N)$ is the ionization frequency for $j = \mathrm{iz}$ and attachment frequency for $j = \mathrm{att}$, respectively. Expression (4.2) contains the relevant physical information of the impedance behaviour. Using relation (4.2) the influence of the temperature of the gas and the detachment frequency ν_{det} on the impedance of the plasma is analysed.

The gas temperature T_g affects the value of the rate coefficients $K_j(E/N)$ for electron collisions in Table 1, because the reduced electric field E/N depends on T_g via the gas density N for a given pressure p_0. Figure 7 shows the influence of the gas temperature on the impedance of the plasma. Qualitative agreement of the theoretical results with the experimental data is found for the entire gas temperature range considered with best quantitative coincidence at temperatures around 420 K. This confirms the estimate (3.8) for the gas temperature and gives a means to estimate the gas temperature independently.

The increasing deviations between measured and calculated impedance values for frequencies above 10 kHz are caused by the fact that the EVDF is no longer in equilibrium with the external electric field so that the assumption $K_j = K_j(E/N)$ for the reaction rate coefficients of electron collision processes begins to break down.

The influence of the detachment frequency ν_{det} on the plasma impedance is illustrated in Fig. 8. Here, results of model calculations for the two values $\nu_{\mathrm{det}} = 166$ and 331 kHz are compared with the experimental data for the frequency range from 0.3 to 40 kHz, where the assumptions made to derive (4.2) are justified. That is, the neutral species O_2^* and O can be considered as quasi-stationary and the electrons are in equilibrium with the variation of the electric field.

https://doi.org/10.1017/S0022377808007502 Published online by Cambridge University Press

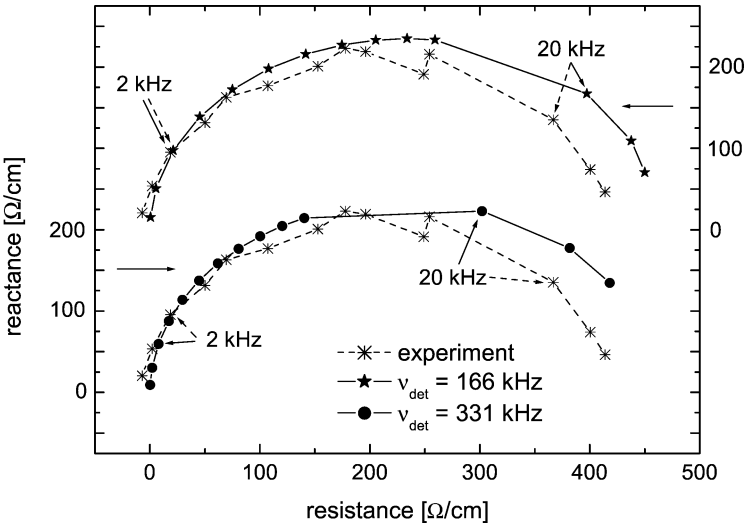

Figure 8. Influence of the detachment frequency ν_{det} on the plasma impedance parameterized by the frequency under standard discharge conditions. Frequency labels from left to right: 300 Hz, $1, 2, \ldots, 9$ kHz and $10, 20, \ldots, 40$ kHz.

The value $\nu_{\mathrm{det}} = 331$ kHz corresponds to a concentration of 7.9% for O_2^* and 2.3% for O at the discharge conditions $p_0 = 0.7$ Torr, $I_0 = 32$ mA and $T_g = 420$ K (see above). At this detachment frequency remarkable discrepancies in the frequency dependence of the theoretical results compared with the measured values are obvious (cf. the lower graph in Figure 8). These differences disappear when reducing the detachment frequency by a factor of two, i.e. $\nu_{\mathrm{det}} = 166$ kHz corresponding to a concentration of the detachment partners of about 6% for O_2^* and O together.

The equilibrium densities of the neutral species as calculated by the balance equations (3.4c) and (3.4d) are very sensitive to, e.g., the inclusion of additional quenching processes for the metastable molecules [27] or the rise of the value of the quenching probability on the wall γ_{m} each resulting in lower concentrations of O_2^*. Unfortunately, experimental data are not available for the densities of atomic oxygen and metastable oxygen molecules at the discharge conditions considered. Using the similarity law [28] the standard discharge condition corresponds to the situation $p_0 = 3$ Torr and $I_0 = 7.7$ mA in [10]. Extrapolating the experimental curves given in [10, Figs. 2 and 3] to the present standard discharge condition a value of about 4% for the concentration of O_2^* and 2% for O is expected. This confirms the predictions of the simplified description of the plasma impedance by means of relation (4.2) and assuming $\nu_{\mathrm{det}} = 166$ kHz.

5. Conclusion

The dynamic behaviour of the positive column plasma of dc discharges in oxygen has been studied using experiments and modelling. Despite the rather complex chemistry of oxygen plasmas its impedance behaviour can be described well by means of a comparatively simple model, in essence by relation (4.2), because the dynamic behaviour of the plasma is governed mostly by the dynamics of the charged particles. Thus, only two electronic reaction rate coefficients are required,

https://doi.org/10.1017/S0022377808007502 Published online by Cambridge University Press

namely the ionization rate coefficient K_{iz} and the attachment rate coefficient K_{att}, for modelling the dynamical plasma behaviour and the rest of the plasma chemistry is contained in the single parameter of the detachment frequency ν_{det}.

The model provides an accurate description of the experimental impedance data for the investigated parameter range of oxygen discharges. It can be utilized to validate the reaction rate coefficients and discharge parameters. An extension of the approach for the analysis of other electronegative plasmas and more general situations is possible.

Acknowledgements

This work was in part supported by the Sonderforschungsbereich TR 24. The authors thank H. Deutsch and B. Bruhn for valuable discussions.

References

[1] Bogdanov, E. A., Kudryavtsev, A. A., Tsendin, L. D., Arslanbekov, R. R., Kolobov, V. I. and Kudryavtsev, V. V. 2003 Scaling laws for the spatial distributions of the plasma parameters in the positive column of a dc oxygen discharge. *Tech. Phys.* **48**, 1151–1158.

[2] Franklin, R. N. 2001 A comprehensive treatment of the positive column of discharges in electronegative gases. *Proc. R. Soc. Lond. A* **457**, 307–330.

[3] Gudmundsson, J. T., Kouznetsov, I. G., Patel, K. K. and Lieberman, M. A. 2001 Electronegativity of low-pressure high-density oxygen discharges. *J. Phys. D: Appl. Phys.* **34**, 1100–1109.

[4] Gudmundsson, J. T. 2004 Recombination and detachment in oxygen discharges: the role of metastable oxygen molecules. *J. Phys. D: Appl. Phys.* **37**, 2073–2081.

[5] Katsch, H. M., Sturm, T., Quandt, E. and Döbele, H. F. 2000 Negative ions and the role of metastable molecules in a capacitively coupled radiofrequency excited discharge in oxygen. *Plasma Sources Sci. Technol.* **9**, 323–330.

[6] Lichtenberg, A. J., Lieberman, M. A., Kouznetsov, I. G. and Chung, T. H. 2000 Transitions and scaling laws for electronegative discharge models. *Plasma Sources Sci. Technol.* **9**, 45–56.

[7] Corr, C. S., Steen, P. G. and Graham, W. G. 2003 Instabilities in an inductively coupled oxygen plasma. *Plasma Sources Sci. Technol.* **12**, 265–272.

[8] Descoeudres, A., Sansonnens, L. and Hollenstein, Ch. 2003 Attachment-induced ionization instability in electronegative capacitive RF discharges. *Plasma Sources Sci. Technol.* **12**, 152–157.

[9] Nighan, W. L. and Wiegand, W. J. 1974 Influence of negative-ion processes on steady-state properties and striations in molecular gas discharges. *Phys. Rev. A* **10**, 922–945.

[10] Belostotsky, S. G., Economou, D. J., Lopaev, D. V. and Rakhimova, T. V. 2005 Negative ion destruction by $O(^3P)$ atoms and $O_2(a^1\Delta_g)$ molecules in an oxygen plasma. *Plasma Sources Sci. Technol.* **14**, 532–542.

[11] Kaganovich, I. D., Ramamurthi, B. N., and Economou, D. J. 2001 Spatiotemporal dynamics of charged species in the afterglow of plasmas containing negative ions. *Phys. Rev. E* **64**, 036402.

[12] Wilke, C., Kablan, N. and Deutsch, H. 1990 On a new method of determining collision rates for ionization by means of pair collisions and stepwise ionization. *Contr. Plasma Phys.* **30**, 481–486.

[13] Phelps, A. V. 1998 Electron Transport Data. ftp://jila.colorado.edu/collision_data.

[14] Raizer, Yu. P. 1997 *Gas Discharge Physics*. Berlin: Springer.

[15] Leyh, H., Loffhagen, D. and Winkler, R. 1998 A new multi-term solution technique for the electron Boltzmann equation of weakly ionized steady-state plasmas. *Comput. Phys. Commun.* **113**, 33–48.

[16] Pinhão, N. R., Donkó, Z., Loffhagen, D., Pinheiro, M. J. and Richley, E. A. 2004 Comparison of kinetic calculation techniques for the analysis of electron swarm transport at low to moderate E/N values. *Plasma Sources Sci. Technol.* **13**, 719–728.

[17] Franklin, R. N. 2001 The role of $O_2(a^1\Delta_g)$ metastables and associative detachment in discharges in oxygen. *J. Phys. D: Appl. Phys.* **34**, 1834–1839.

[18] Ellis, H. W., Pai, R. Y., McDaniel, E. W., Mason, E. A. and Viehland, L. A. 1976 Transport properties of gaseous ions over a wide energy range. *Atomic Data Nucl. Tables* **17**, 177–210.

[19] Viehland, L. A. and Mason, E. A. 1995 Transport properties of gaseous ions over a wide energy range, IV. *Atomic Data Nucl. Tables* **60**, 37–95.

[20] Ferreira, C. M., Gousset, G. and Touzeau, M. 1988 Quasi-neutral theory of positive columns in electronegative gases. *J. Phys. D: Appl. Phys.* **21**, 1403–1413.

[21] Franklin, R. N. and Snell, J. 1999 Modelling discharges in electronegative gases *J. Phys. D: Appl. Phys.* **32**, 2190–2203.

[22] Gousset, G., Touzeau, M., Vialle, M. and Ferreira, C. M. 1989 Kinetic model of a dc oxygen glow discharge. *Plasma Chem. Plasma Proc.* **9**, 189–206.

[23] Sabadil, H. and Pfau, S. 1985 Measurements of the degree of dissociation in oxygen dc discharges: comparison of the ozone method with the Wrede–Harteck method. *Plasma Chem. Plasma Proc.* **5**, 67–79.

[24] Klopovskiy, K. S., Lopaev, D. V., Popov, N. A., Rakhimov, A. T. and Rakhimova, T. V. 1999 Heterogeneous quenching of $O_2\,{}^1\Delta_g$ molecules in H_2:O_2 mixtures. *J. Phys. D: Appl. Phys.* **32**, 3004–3012.

[25] Touzeau, M., Vialle, M., Zellagui, A., Gousset, G., Lefebvre, M. and Pealat, M. 1991 Spectroscopic temperature measurements in oxygen discharges. *J. Phys. D: Appl. Phys.* **24**, 41–47.

[26] Sabadil, H. 1966 Die Schichterscheinungen in der positiven Säule der Sauerstoff-Niederdruckentladung. *Beitr. Plasmaphys.* **6**, 305–317.

[27] Gousset, G., Ferreira, C. M., Pinheiro, M., Sa, P. A., Touzeau, M., Vialle, M. and Loureiro, J. 1991 Electron and heavy-particle kinetics in the low pressure oxygen positive column. *J. Phys. D: Appl. Phys.* **24**, 290–300.

[28] Pfau, S., Rutscher, A. and Wojaczek, K. 1969 Das Ähnlichkeitsgesetz für quasineutrale, anisotherme Entladungssäulen. *Beitr. Plasmaphys.* **9**, 333–358.